The development of 1 MW ECRH system on J-TEXT

Xixuan Chen[1], *Donghui* Xia[1,*], *Junli* Zhang[1], *Zhijiang* Wang[1], *Yuan* Pan[1] and J-TEXT team[1]

[1]International Joint Research Laboratory of Magnetic Confinement Fusion and Plasma Physics, Huazhong University of Science and Technology, 430074 Wuhan, China

Abstract. A 1 MW electron cyclotron resonance heating system has been designed and developed for J-TEXT tokamak not only to enhance the total heating power but also to provide another possible way to control the plasma parameters. The system is composed of two gyrotrons, both with an output power of 500 kW electron cyclotron wave power. The development progress of the system is elaborated and discussed. The commissioning tests for the gyrotrons were implemented, and each gyrotron realized its standard output successfully. With the assistance of this system, a variety of experiments have been carried out on J-TEXT, mainly related to plasma heating, plasma disruption, plasma start-up, current drive and so on.

1 Introduction

With advantages like highly localized power deposition and high coupling efficiency, electron cyclotron resonance heating (ECRH) has been widely applied on many magnetic confinement fusion devices (e.g., DIII-D, W7-X, HL-2A) [1-3] and is considered to be used for future fusion demonstration reactors. In order to improve the plasma parameters and broaden the operation range of Joint-TEXT (J-TEXT) tokamak, the development of the ECRH system has been initiated in 2017. After the integration design and setup of subsystems, a gyrotron which is at a frequency of 105 GHz with a power of 500 kW for 1 s was tested and put into physical experiments in 2019. Another gyrotron of same parameters has just finished its commissioning tests in 2022. Therefore, the J-TEXT ECRH system could realize an output power of 1 MW in total. The layout of the ECRH system is shown in Fig. 1 [4].

This paper is organized as follows. The introduction of the 1 MW ECRH system on J-TEXT is presented in section 2. The gyrotron commissioning tests are presented and discussed in section 3. The related physical experiments are presented in section 4.

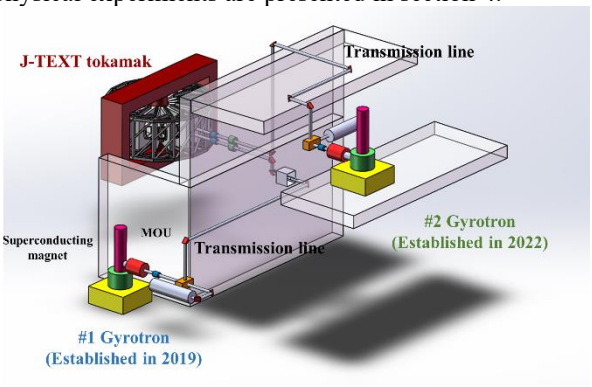

Fig. 1. Layout of J-TEXT 1 MW ECRH system

2 J-TEXT ECRH system

The J-TEXT tokamak is a conventional iron core tokamak reconstructed from the Texas Experimental Tokamak Upgrade (TEXT-U) [5-7]. The basic operation parameters of J-TEXT are listed in Table 1. As a long-term research program, the J-TEXT is aimed at developing fundamental physics and control mechanisms of high-temperature tokamak plasma confinement and stability.

Table 1. Basic operation parameters of J-TEXT.

Parameters	Value
Major radius (R_0)	1.05 m
Minor radius (a)	25-29 cm
Toroidal field (B_t)	<2.4 T
Plasma current (I_p)	<240 kA
Plasma densities (n_e)	(1-7)×10^{19} m^{-3}
Electron temperatur (T_e) (With ohmic heating)	~1 keV

The ECRH system has been developed for J-TEXT to increase the core electron temperature and also to study the non-inductive current drive. This system is designed to work at the X2 mode for plasma heating and non-inductive current drive, considering its practical application.

* Corresponding author: xiadh@hust.edu.cn

As the core component of ECRH system, the gyrotron generates high power microwave of special frequency during a long pulse. The J-TEXT ECRH system contains two gyrotrons of 500 kW power each which are both manufactured by GYCOM Ltd., so in total the ECRH system could realize an output of 1 MW. The main characteristic parameters are given in Table 2. The first gyrotron finished its commissioning tests and was put into formal operation in J-TEXT physical experiments since 2019. The commissioning tests of the second gyrotron were just finished in 2022.

Table 2. Main characteristic parameters of the gyrotrons for J-TEXT ECRH system.

Parameters	Value (#1 gyrotron)	Value (#2 gyrotron)
Frequency	105 GHz	105 GHz
Maximum output power	500 kW	500 kW
Maximum pulse duration	1 s	1 s
TEM_{00} mode purity (after MOU)	97%	98%
Output efficiency	45%	45%

Each gyrotron is equipped with a set of subsystems to realize its safe and stable operation, Fig. 2 shows the corresponding diagram.

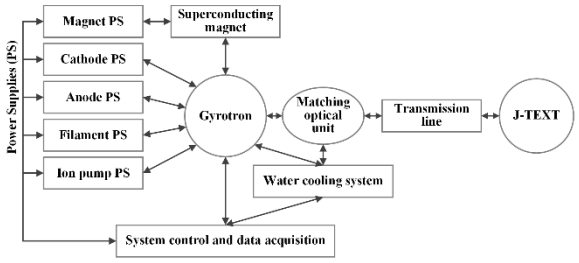

Fig. 2. Diagram of gyrotron operation platform.

There are various power supplies (PS) indispensable for gyrotron operation. Two high voltage power supplies which are the cathode power supply and anode power supply provide high voltage for establishing an accelerating electric field inside the gyrotron. Besides, to make the electrons form a helical motion, the superconducting magnet is needed to build a steady-state magnetic field, thus the magnet power supply is used to charge the superconducting magnet. What is worth mentioning here is that the superconducting magnet for the first gyrotron is cooled by liquid helium and nitrogen while the magnet for the second is cryogen-free. The filament power supply is used to heat the filament inside the gyrotron in order to generate active electrons. The ion pump power supply could maintain the vacuum of the gyrotron, which is very important for its operation. The electrical parameters of the power supplies are listed in Table 3.

Table 3. Electrical parameters of power supplies for the gyrotron.

Power supply	Parameters (#1 gyrotron)	Parameters (#2 gyrotron)
Cathode power supply	-44 kV/25 A	-45 kV/24 A
Anode power supply	30 kV/150 mA	32 kV/200 mA
Magnet power supply	100 A	100 A
Ion pump power supply	5 kV/10 mA	5kV/10 mA
Filament power supply	1500 VA	2500 VA

In addition to the power supplies, there is a specially designed control system for the gyrotron. The control system realizes functions including time sequence trigger, data acquisition, communication and most noteworthy, protection [8]. Besides, the ECRH system should be equipped with a cooling system to cool down the crucial components and meanwhile measure the output microwave power.

The subsystems mentioned above work together with the gyrotron in order to generate microwave as desired. The output microwave is then corrected by the mirrors in matching optical unit (MOU) which is connected with the output window of the gyrotron. To realize localized and efficient plasma heating, a specialized transmission line is constructed to guide the microwave into the plasma. The transmission line is mainly composed of corrugated waveguide, mitre bend, DC break and launcher [9], which are designed combining the characteristics of the output microwave. The transmission loss is mainly caused at mitre bends. There is either flat mirror or polarizer on each bend. The amount of these components and the possible transmission loss caused by them is listed in Table 4.

Table 4. The number of flat mirrors and polarizers and their possible transmission loss

Component	Number	Possible transmission loss
Flat mirror	3	1%~2%
Polarizer	2	2%~3%
Total		7%~12%

3 Commissioning tests of gyrotron

Before carrying out related physics experiments on J-TEXT tokamak, commissioning tests of the two gyrotrons are ought to be finished to check their status and to explore their operation characteristics.

The commissioning of a gyrotron usually contains the following stages. The first stage is cooling down of

magnet in order to bring it to the superconducting state. The second stage is the alignment of the magnet, because the axis of the gyrotron should coincide that of the magnet. The third stage is gyrotron operation to find its best operation condition. Along with the gyrotron operation, MOU installation and alignment should be carried out in order to focus and direct the microwave beam correctly after it leaves the gyrotron. The final stage of the commissioning is also the most crucial part, that is to adjust all control parameters to increase gyrotron output power to the maximum value.

3.1 Cooling down of the magnet

As for magnet cooling, the temperature and magnet resistance change of the whole process is recorded, shown in Fig. 3. Fig. 3 (*a*) shows the resistance change and Fig. 3 (*b*) shows the temperature change. At the end of the cooling down process, the magnet resistance is 0.05 Ω and its temperature reached 3 K.

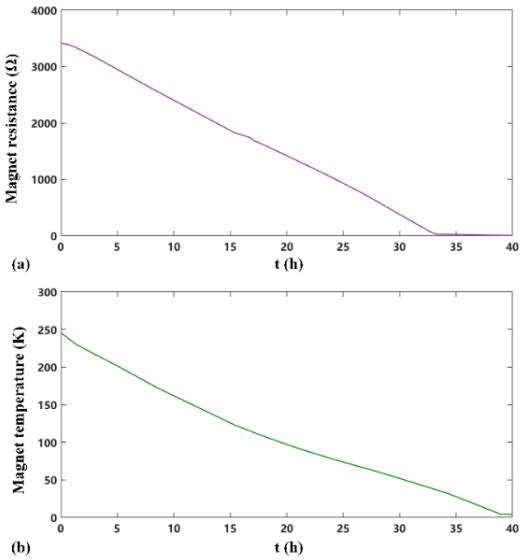

Fig. 3. Magnet resistance change (*a*) and magnet temperature change (*b*) during the cooling down process.

3.2 Magnet alignment

The magnet alignment is also very crucial and needs to be implemented precisely [10]. Without good alignment, there is a great chance that the gyrotron couldn't reach its best working condition, especially when a high-power output is required. The target of this step is to make the axis of the magnet coincide with that of the gyrotron as much as they could. That is to say, in this step, the higher the degree of two axes coincide with each other, the better alignment we have obtained. Figure. 4 shows the diagram of poor magnet alignment and good magnet alignment. A dummy tube which has a window to observe the fluorescent ring formed by electrons is used to replace the gyrotron in this step and its size is exactly the same as the gyrotron. When a fluorescent ring looks like orbit 1 in Fig. 4, it means good alignment has been obtained. While a fluorescent ring like orbit 2 takes place, more adjustment work should be done.

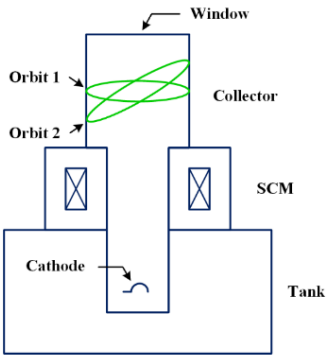

Fig. 4. Diagram of poor and good magnet alignment.

3.3 Gyrotron operation

The gyrotron could be operated without MOU at first to realize an output of low power and relatively low mode purity. Through this we could find a combination of suitable parameters for the gyrotron, which is also beneficial for MOU alignment.

Generally, the MOU contains a pair of phase correcting mirrors, the internal structure of which is shown in Figure. 5. To design an MOU for a gyrotron, the initial output wave of the gyrotron should be measured. Then the MOU is designed according to the actual output of the gyrotron.

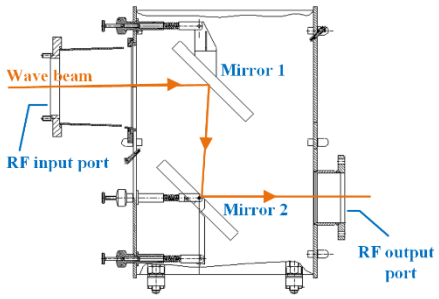

Fig. 5. Internal structure of MOU.

The most crucial goal of the commissioning is to find the most appropriate operation status for the gyrotron [11]. There are a few parameters that could have an influence on the gyrotron operation status, of them the most important are the magnet field intensity, the filament power, the cathode voltage and anode voltage. Besides understanding how those parameters could affect the gyrotron operation status, it is also very important to think out how to evaluate its operation status. Three ways are used to realize this target. The first is to build up a platform to measure the microwave signal, which is also called radio frequency (RF) signal and is obtained by directional coupler method [12]. The second is to use a spectrometer to measure the frequency of the output wave. The third is to measure its power with a dummy load, this method is called calorimetric method [13]. If the measured RF signal, frequency spectrum signal and output power are basically the same as results in the factory tests, then the gyrotron operation status is quite standard and good. Figure. 6 shows the measured RF signal and Fig. 7 gives the temperature rise

curve which is used to calculate the microwave power. The area of the temperature rise curve represents the energy absorbed by cooling water. To calculate the microwave power, we first used a power supply with known power to heat the water, with formula (1) we could then calculate the microwave power because the pulse width of microwave is also clear.

$$P_{rf} = P_k \frac{D_k S_{rf}}{D_{rf} S_k} \quad (1)$$

here, P_k is the power of the power supply, D_k is the pulse width of the electric power, S_{rf} is the area of the measured temperature rise curve when the microwave is absorbed by the water, D_{rf} is the pulse width of the microwave power, and S_k is the area of the measured temperature rise curve of the electric power.

As for the calibration of the RF-signal, the gyrotron should be operated under same parameters for 2 shots, and the microwave power are measured by calorimetric method and directional coupler method separately. The amplitude of the output signal from directional coupler method varied with different microwave power. The calculation results of calorimetric method could be used to calculate the RF-signal measured by directional coupler method.

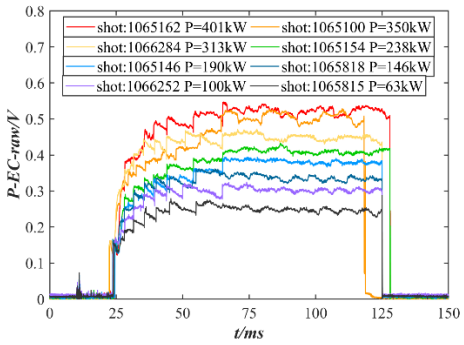

Fig. 6. Measured RF signal during gyrotron operation. Different shot has different power, therefore the RF signal has different value.

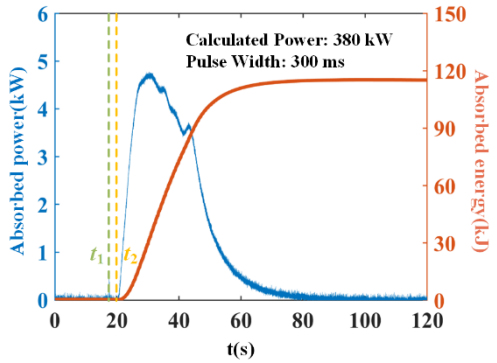

Fig. 7. A typical temperature rise curve during gyrotron operation, the left axis represents the power absorbed by water and the right axis represents the absorbed energy. Calculated power is 380 kW and the pulse width is 300 ms. t_1 is the microwave injection time while t_2 is the temperature rising time.

Through exploring the working characteristics of the gyrotron, its control parameters could be optimized continuously. Here a typical shot of one pulse is given in Figure. 8. In this shot, the cathode voltage is -40 kV, the anode voltage is 22 kV and the cathode current is 22 A, which corresponds to an output of 350 kW microwave power. Both gyrotrons have realized their maximum output power, however, considering the operation stability and safety, they are usually operated no more than 80% of the maximum output power.

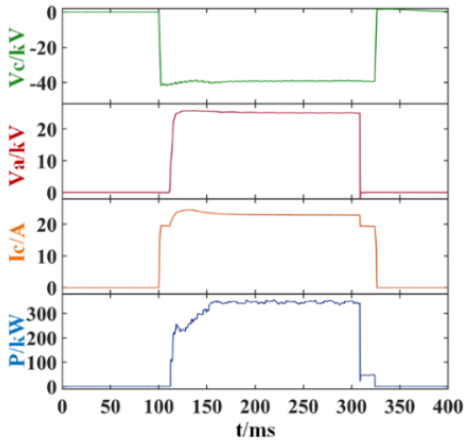

Fig. 8. Waveforms of a typical shot.

4 The experimental results with ECRH

The first gyrotron has been utilized in J-TEXT physical experiments right after the commissioning tests were finished. The microwave generated by the gyrotron was successfully injected into J-TEXT in 2019. The second gyrotron is not in use formally now because the commissioning tests were just finished recently. Until now, various kinds of related experiments have been carried out on J-TEXT, related to not only plasma heating but also plasma disruption, sawtooth control, plasma start-up, current drive and so on.

4.1 Electron thermal transport and temperature fluctuations of ECRH

Dedicated experiments have been carried out on the J-TEXT for investigating the electron thermal transport and plasma fluctuations before and during electron cyclotron resonance heating.

Fig. 9 [13] shows a typical discharge with ECRH for shot #1069645. The main plasma parameters are shown in Table 5.

Table 5. Main plasma parameters of shot #1069645

Parameters	Value
B_t	1.875 T
I_p	175 kA
n_e	(2-2.5)×10^{19} m^{-3}

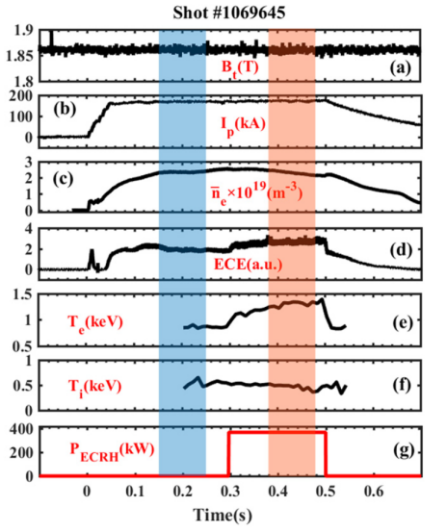

Fig. 9. Time evolution of plasma parameters for shot 1069645: (*a*) toroidal field B_t; (*b*) plasma current I_p; (*c*) line-averaged electron density $\bar{n}_e$; (*d*) electron temperature at r/a = 0.72 by ECE (no calibration); (*e*)-(*f*) the core of plasma electron and ion temperature obtained by XICS; (*g*) the ECRH power [14].

In Fig. 9, both the electron temperature at r/a = 0.72 measured by the electron cyclotron emission (ECE) diagnostic (Fig. 9(*d*)) and the core of electron temperature from the x-ray imaging crystal spectrometer (XICS) (Fig. 9(*e*)) increase significantly during ECRH. The core ion temperature (Fig. 9(*f*)) does not increase as the electron temperature but decreases with ECRH. The decrease of ion temperature in the plasma core indicates that ion heat transport may be enhanced.

4.2 Fast electron with ECCD

Fast electrons could be generated by electron cyclotron wave through wave-particle interaction when the resonant condition is fulfilled. The fast electron bremsstrahlung diagnostic on J-TEXT enables detailed studies of the generation and transport of fast electrons.

When the toroidal field is 1.875 T, the electron cyclotron wave absorption area is on-axis according to the calculation. A typical on-axis electron cyclotron current drive (ECCD) experiment with a number of fast electrons is shown in Fig. 10 [14]. In this shot, the plasma current is 150 kA, central electron density is kept at about 1×10^{19} m^{-3}. With the EC wave injection at 250 ms, the line integrated intensity signal from the central chord of FEB IFEB begins to rise (Fig. 10(c)). The ECE signals at 80.5 GHz which the resonance layer is outside the plasma (+31.96 cm) are dominated by relativistically downshifted emission by the high-energy tail of the electron distribution function and can be employed to diagnose the population of fast electrons, as shown by the black line in Fig. 10(e).

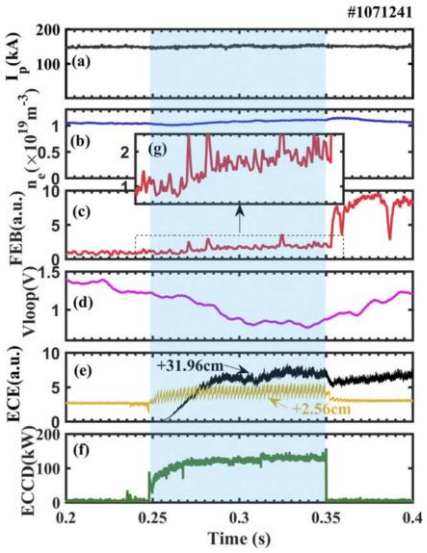

Fig. 10. Temporal evolution of typical on-axis ECCD experiment which generated a large number of fast electrons [15]. From the top to bottom, the waveforms are: (a) the plasma current, (b) the central line averaged electron density, (c) FEB signal at the radial position of 0 cm (from demodulator), (d) the loop voltage, (e) ECE signals at the radial position of +2.56 cm and +31.96 cm (out of plasma), (f) ECCD power. About 150 kW EC wave power is injected into plasma from 250 ms to 350 ms and (g) the enlarged FEB signal of dashed box.

5 Summary

J-TEXT 1 MW ECRH system contains 2 gyrotrons of 105 GHz/500 kW/1 s which are manufactured by GYCOM. The first gyrotron was tested and put into operation in 2019. The commissioning tests of the second gyrotron is just finished in 2022. During the commissioning process of the gyrotron, the cooling down and alignment of the magnet, the MOU alignment and the gyrotron operation were finished. The high power and long pulse output has been realized during the commissioning tests. Since 2019, the first gyrotron has been utilized in J-TEXT physical experiments, which not only expanded the parameter range of J-TEXT, but also promoted the ECRH and ECCD related research.

ACKNOWLEDGMENTS

The authors want to appreciate J-TEXT team for valuable discussion and suggestion about electron cyclotron resonance heating. This work was supported by the National Key Research and Development Program of China (Grant 2017YFE0300200 and Grant 2017YFE0300204), the Key Research and Development Program of Hubei province (Grant 2021BAA167) and the National Natural Science Foundation of China (Grant 51821005).

References

1. M. Cengher, J. Lohr, Y. A. Gorelov, R. Ellis, Egemen Kolemen, D. Ponce, S. Noraky, C. P. Moeller, IEEE Trans. Plasma Sci. **42**, 7 (2014)
2. W. Kasparek, P. Brand, H. Braune, G. Dammertz, V. Erckmann, G. Gantenbein, F. Hollmann, M. Grünert, H. Kumric, L. Jonitz, H.P. Laqua, W. Leonhardt, G. Michel, F. Noke, B. Plaum, F. Purps, M. Schmid, T. Schulz, K. Schwörer, M. Thumm, M. Weissgerber, Fusion Eng. Des. **74**, 243 (2005)
3. M. Huang, J. Rao, B. Li, J. Zhou, Z.H. Kang, H. Wang, B. Lu, D.H. Xia, C. Wang, K. Feng, M.W. Wang, G.Y. Chen, Y.N. Pu, Z.H. Lu, J.Q. Wang, X.R. Duan, Y. Liu, in Proceedings of the 17th Joint Workshop on Electron Cyclotron Emission and Electron Cyclotron Resonance Heating, 7-10 May 2012, Deurne, Netherlands (2012)
4. J.L. Zhang, D.H. Xia, C.H. Liu, Z.J. Wang, Y. Pan, IEEE Trans. Plasma Sci. **48**, 6 (2020)
5. Y. Liang, N.C. Wang, Y.H. Ding, Z.Y. Chen, Z.P. Chen, Z.J. Yang, Q.M. Hu, Z.F. Cheng, L. Wang, Z.H. Jiang, B. Rao, Z. Huang, Y. Li, W. Yan, D. Li, H. Liu, L. Zeng, Y. Huang, D.W. Huang, Z.F. Lin, W. Zheng, F.R. Hu, K.J. Zhao, M. Jiang, Y.J. Shi, H. Zhou, S.T. Peng, W.X. Guo, L. Gao, Z.J. Wang, M. Zhang, K.X. Yu, X.W. Hu, Q. Yu, G. Zhuang, K.W. Gentle, Y. Pan, the J-TEXT Team, Nucl. Fusion **59**, 112016 (2019)
6. G. Zhuang, Y. Pan1, X.W. Hu, Z.J. Wang, Y.H. Ding, M. Zhang, L. Gao, X.Q. Zhang, Z.J. Yang, K.X. Yu, K.W. Gentle, H. Huang, the J-TEXT Team, Nucl. Fusion **51**, 094020 (2011)
7. Y.H. Ding, Z.Y. Chen, Z.P. Chen, Z.J. Yang, N.C. Wang, Q.M. Hu, B. Rao, J. Chen, Z.F. Cheng, L. Gao, Z.H. Jiang, L. Wang, Z.J. Wang, X.Q. Zhang, W. Zheng, M. Zhang, G. Zhuang, Q.Q. Yu, Y.F. Liang, K.X. Yu, X.W. Hu, Y. Pan, K.W. Gentle, the J-TEXT team, Plasma Sci. Technol. **20**, 125101 (2018)
8. Z. Wang, G. Fan, D. Xia, X. Chen, W. Weng, IEEE Trans. Plasma Sci. **49**, 258 (2021)
9. J.L. Zhang, D.H. Xia, C.H. Liu, Z.J. Wang, Y. Pan, IEEE Trans. Plasma Sci. **48**, 1560 (2020)
10. D.H. Xia, M. Huang, J. Zhou, X.Y. Bai, T.L. Zheng, J. Rao, G. Zhuang, Plasma Sci. Technol. **16**, 410 (2014)
11. H. Wang, J. Rao, M. Huang, J. Zhou, C. Wang, Z.H. Kang, M.W. Wang, K. Feng, G.Y. Chen, B. Lu, J.Q. Wang, Fusion Eng. Des. **101**, 61 (2015)
12. T. Notake, H. Idei, S. Kubo, T. Shimozuma, Y. Yoshimura, S. Kobayashi, Y. Mizuno, S. Ito, Y. Takita, K. Ohkubo, W. Kasparek, T. Watari, R. Kumazawa, Rev. Sci. Instrum. **76**, 023504 (2005)
13. G. Michel, H. Laqua, W. Kasparek, Fusion Eng. Des. **56-57**, 655 (2001)
14. Z.J. Yang, Y.P. Zhang, X.H. Ren, F. Li, X. Xu, W. Yan, X.Y. Zhang, D.H. Xia, Z.C. Zhang, Y. Gao, X.Q. Zha, Q. Luo, Z.Y. Chen, Z.F. Cheng, Z.P. Chen, L. Gao, Y.H. Ding, Nucl. Fusion **61**, 086005 (2021)
15. X.B. Zhang, W. Yan, Z.Y. Chen, J.G. Fang, J.L. Zhang, Y. Li, X.X. Chen, Y.N. Wei, R.H. Tong, Z.F. Lin, Y. Zhong, L.K. Mou, F. Li, Z.H. Jiang, Z.J. Yang, N.C. Wang, Y. Pan, the J-TEXT team, Plasma Sci. Technol. **24**, 064007 (2022)